JOURNAL OF GEOPHYSICAL RESEARCH, VOL. 101, NO. D4, PAGES 9031–9043, APRIL 20, 1996

Simultaneous measurements of stratospheric HO_x, NO_x, and Cl_x: Comparison with a photochemical model

K. Chance, W.A. Traub, D.G. Johnson, K.W. Jucks, and P. Ciarpallini

Harvard-Smithsonian Center for Astrophysics, Cambridge, Massachusetts

R.A. Stachnik

Jet Propulsion Laboratory, California Institute of Technology, Pasadena, California

R.J. Salawitch[1] and H.A. Michelsen

Department of Earth and Planetary Sciences, Harvard University, Cambridge, Massachusetts

Abstract. We report simultaneous measurements of the stratospheric concentration profiles of OH, HO_2, H_2O_2, H_2O, O_3, HNO_3, NO_2, N_2O, HCl, HOCl, and ClO during a midlatitude balloon flight in 1989. Measurements were made over almost an entire diurnal cycle by the Smithsonian Astrophysical Observatory Far-Infrared Spectrometer (FIRS-2) and the Jet Propulsion Laboratory Balloon Microwave Limb Sounder (BMLS). We analyze these measurements using a photochemical model constrained by observations of long-lived gases. Measured HO_x species (OH and HO_2) and H_2O_2 show fair agreement with theory throughout the diurnal cycle. Measurements of HNO_3 are higher than theory near the concentration peak, while the levels of NO_2 are consistent with the model at most altitudes. Measurements of ClO and HOCl are less than predicted concentrations, suggesting a source of HCl in addition to the reaction of Cl with CH_4. Possibilities for such a source include a minor HCl + O_2 product channel for the reaction of ClO with OH and a minor HCl + O_3 channel for the reaction of ClO with HO_2.

Introduction

Catalytic destruction of ozone from the HO_x, Cl_x, and NO_x reaction cycles is a central feature of the chemistry of the Earth's ozone layer. However, it has been difficult to obtain simultaneous measurements of these radical species and their reservoirs over a range of altitudes. We report the first simultaneous measurement of HO_x, Cl_x, and NO_x species throughout the middle atmosphere. These observations represent the most comprehensive description yet obtained of the distribution of free radicals and photochemically related gases involved in catalytic destruction of ozone.

Stratospheric balloon platforms carrying several instruments are effective at making simultaneous measurements of multiple species. The molecules currently measured by the FIRS-2 instrument include OH, HO_2, H_2O_2, H_2O, O_3, O_2, O^3P (in the mesosphere and thermosphere), HCl, HF, HOCl, HBr, CO_2, HNO_3, NO_2, N_2O, CO, HCN, and CO_2 (temperature and pressure profiles are derived from the 16-μm bands of CO_2). The Balloon Microwave Limb Sounder (BMLS) instrument measures ClO and O_3. In this paper we concentrate on measurements of HO_x (OH and HO_2), the closely related H_2O_2, and the Cl_y and NO_y species ClO, HOCl, HCl, NO_2, and HNO_3. Measurements of radical precursors H_2O, O_3, and N_2O and temperature are used to constrain the photochemical model calculations as described below.

Measurements of the species considered in this analysis have been described in the literature. OH has been measured in the stratosphere using balloon-borne far-infrared thermal emission spectroscopy [*Kendall and Clark*, 1980; *Traub et al.*, 1991; *Carli et al.*, 1989; *Park and Carli*, 1991; *Pickett and Peterson*, 1993], in situ resonance fluorescence [*Stimpfle et al.*, 1990; *Wennberg et al.*, 1990, 1994], and balloon-borne lidar [*Heaps et al.*, 1985]. Ground-based measurements that include the stratospheric content as a part of the total column have also been made [*Burnett et al.*, 1988; *Iwagami et al.*, 1995]. The measurements presented here are the first to include the altitude profile in the stratosphere and its time variation through most of a diurnal cycle.

[1]Now at Jet Propulsion Laboratory, California Institute of Technology, Pasadena, California

Paper number 96JD00064.
0148-0227/96/96JD-00064$05.00

HO_2 has been measured in remote sensing by balloon-borne far-infrared thermal emission spectroscopy [*Traub et al.*, 1990; *Park and Carli*, 1991] and submillimeter heterodyne spectroscopy [*Stachnik et al.*, 1992] and by ground-based millimeter-wave spectroscopy [*de Zafra et al.*, 1984]. HO_2 has also been measured in situ with two techniques: chemical conversion followed by resonance fluorescence [*Anderson et al.*, 1981; *Stimpfle et al.*, 1990; *Wennberg et al.*, 1994] and matrix isolation followed by ESR spectroscopic analysis [*Helten et al.*, 1984]. H_2O_2, which is photochemically closely related to OH and HO_2, has only been measurable in the stratosphere using far-infrared thermal emission spectroscopy [*Chance and Traub*, 1987; *Chance et al.*, 1991; *Park and Carli* 1991]. Stratospheric NO_2 has been well determined by using infrared and visible measurement techniques [*Roscoe et al.*, 1990; *Russell et al.*, 1988; *Webster et al.*, 1990]; to our knowledge the present study is the first quantitative determination of its concentration profile using far-infrared emission spectroscopy. Concentrations of H_2O, O_3, HNO_3, N_2O, and HCl have been measured by a number of investigators; reviews of most techniques for the measurement of these gases can be found in the reports of the *World Meteorological Organization (WMO)* [1986, 1989]. HOCl has been measured in far-infrared thermal emission [*Chance et al.*, 1989] and in infrared solar absorption [*Toon et al.*, 1992]. ClO has been measured by remote sensing from balloon platforms [*Stachnik et al.*, 1992] and the Upper Atmosphere Research Satellite [*Waters et al.*, 1993], by in situ experiments from balloons [*Dessler et al.*, 1993] and aircraft [*Avallone et al.*, 1993] and by ground-based millimeter-wave spectroscopy [*de Zafra et al.*, 1987; *Emmons et al.*, 1995].

The strength of this set of measurements is the simultaneous observation of a large number of individual species, covering a large range of altitudes in the stratosphere and nearly one full diurnal cycle. The completeness of the data set provides a basis for examining our understanding of processes that regulate the partitioning of radicals using a photochemical model constrained by observations of the longer-lived radical precursors.

Balloon Observations

The observations discussed in this paper were made during a balloon flight from Fort Sumner, New Mexico (34°N, 104°W) on September 26, 1989. The balloon reached the float altitude of 36 km at 1105 mountain daylight time (MDT) and began a gradual descent at 1235 MDT on September 27. The flight was terminated at 1426 MDT. No data were recorded from 0430 to 0801 because of a telemetry problem. The spectra included in this study were taken mostly with the telescope pointing to 15°±3° in geographic azimuth, corresponding to an average sampling latitude of 37.0°N, with the later afternoon scans on September 26 pointing to 188°±3°, corresponding to an average sampling latitude of 31.8°N. Solar zenith angles corresponding to the measurement locations that are calculated below include these offsets in the sampling latitude from the actual location of the gondola.

The Smithsonian Astrophysical Observatory (SAO) FIRS-2 instrument was designed specifically to make thermal emission measurements of the stratosphere from a balloon platform. Its capabilities have been described previously [*Traub et al.*, 1991; *Johnson et al.*, 1995a]. Briefly, it is a two-beam, high-resolution (0.004 cm^{-1} unapodized) Fourier transform spectrometer, which measures thermal emission in the far-infrared (80-210 cm^{-1}) and mid-infrared (350-700 cm^{-1}). Measurements are made at various angles above the Earth's limb, with absolute pointing referenced to an accelerometer- and gyroscope-stabilized single-axis platform. Most observations with the FIRS-2 were made using a standard limb-scan sequence, which included blackbody calibration spectra, high-elevation spectra, and measurements at 0° elevation followed by measurements at elevation angles corresponding to five successive 4 km altitudes below the gondola float height. These measurements took place in a time sequence that included 6 min of integration time (two complete spectra) at each angle. Thus each complete limb-scan sequence took approximately 48 min. The results presented here are from both the daytime and the nighttime portions of the flight.

The BMLS is a remote sensing heterodyne radiometer measuring thermal emission spectra near 205 GHz [*Waters et al.*, 1984]. The data presented here are an average of the data taken from 1100 to 1600 MDT on September 26, 1989. The BMLS was oriented on the gondola to view in the same azimuth direction as the FIRS-2 instrument.

Data Analysis and Results

FIRS-2 spectra are analyzed to obtain concentration profiles using the nonlinear least squares fitting procedure developed at the SAO [*Johnson et al.*, 1995a] and the SAO92 spectral line database [*Chance et al.*, 1994]. Retrievals are based on multilayered, curved shell atmospheric models using distributions of pressure and temperature derived from radiosonde data obtained in the vicinity of the balloon flight. The temperature and pressure profiles are refined by fitting selected temperature- and pressure-sensitive portions of the 16-μm bands of CO_2. A comprehensive search for suitable spectral lines of each species has been carried out based upon line intensities, accuracy of spectral line parameters, and freedom from spectral interference. The selection includes eight lines of OH which are above the FIRS-2 noise equivalent width detection limit of $\sim 10^{-5}$ cm^{-1} (hyperfine components are not counted as separate lines here, although they are fully included in the radiative transfer calculations), twenty-seven lines of HO_2, the $^RQ_5$ branch of the lowest H_2O_2 rotational-torsional band, six lines of H_2O, thirty-six lines of O_3, thirty-three lines of NO_2, seven lines of HCl, twenty-two fitting windows, including the Q_2 and Q_4 branches, of HOCl, and numerous lines contained in seventeen fitting windows in

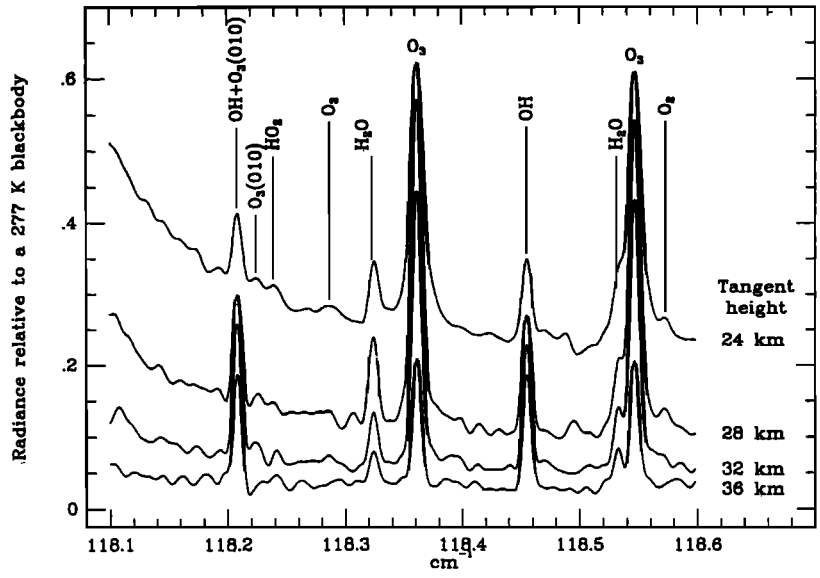

Figure 1. Portions of a single limb-scan sequence (6 min of integration time per spectrum) for the best features of OH in the far-infrared spectrum, the $F_1, 7/2 \leftarrow F_1, 5/2$ lines at 118 cm^{-1}. Spectral transitions with significant intensity are identified. The limb-scan sequence shown is from September 26, 1989, centered in time at 1128 MDT.

the ν_9 vibrational band of HNO_3 and twenty-two fitting windows in the ν_2 vibrational band of N_2O. As an example of the quality of spectra obtained in this balloon flight, Figure 1 shows portions of a single limb scan (6 min of integration time per spectrum) containing the best features of OH in the far-infrared spectrum, the $F_1, 7/2 \leftarrow F_1, 5/2$ lines at 118 cm^{-1}. Spectral transitions with significant intensity are identified in the figure.

Most of the molecules measured here have altitude distributions that permit the onion-peeling retrieval process to proceed in a well-behaved fashion. Their mixing ratios are either nearly constant or decrease with increasing height above the balloon gondola. More importantly, the total amount of gas overhead is sufficiently small that the actual shape of the overhead distribution has a negligible effect on the retrieved concentrations from measurements taken at elevation angles corresponding to measurement heights below the gondola altitude.

The molecules whose concentrations increase with altitude above the gondola height, OH and HO_2 for the FIRS-2 measurements, present a greater challenge in the retrieval process because of the potential for the shape of the overhead distribution to affect concentrations retrieved at lower altitudes. This is particularly true because FIRS-2 does not fully resolve molecular lines, which have widths that are $\sim 3 \times 10^{-4}$ cm^{-1} at 40 km and decrease with increasing altitude. The effect of the shape of the overhead distribution on retrieved concentrations is investigated by assuming overhead distributions highly skewed with respect to standard model profiles (M. Allen, private communication, 1990). Overhead profile shapes affect the derived OH and HO_2 by 6% or less for the 0° elevation angle measurements when the mesospheric concentrations of OH and HO_2 relative to the concentrations at gondola altitude are changed by as much as 25% from the values in the standard distributions. The effects on measurements made at lower-elevation angles are negligible. Line of sight column densities for OH and HO_2 are calculated using an initial-guess model profile for the molecule to be fitted and an altitude step size of 0.1 km. The fitting procedure then scales the initial profile using a retrieval grid matched to the viewing angles.

The FIRS-2 data in this study include a total of 24 limb-scan sequences: 9 from the first day of the flight (1105-1818 MDT), 3 from the second day (1011-1235 MDT), and 12 during the night (2028-0337 MDT). OH and HO_2 retrievals are performed for sums of three successive limb-scan sequences during the daytime for use in comparison with photochemical modeling predictions. The limitation to sums of three limb-scan sequences is caused by the low signal to noise ratios of the measured HO_2 lines; OH can be determined well from individual limb-scan sequences. All other molecules are analyzed by making separate averages of (1) all 9 limb-scan sequences obtained on September 26, (2) all 12 limb-scan sequences obtained during the nighttime, and (3) the first 3 limb-scan sequences obtained on September 27 (the same sum of limb scans coadded for OH and HO_2 retrieval on the morning of September 27). We do not see evidence for diurnal variation of H_2O_2, H_2O, O_3, HNO_3, N_2O, and HCl, which have long photochemical lifetimes. Our measurement sensitivity is sufficient to distinguish between the average daytime and the average nighttime concentrations for NO_2 and HOCl but not to determine their diurnal variation on a finer timescale.

ClO was measured by the BMLS instrument, which

Table 1. Retrieved FIRS-2 Mixing Ratio Profiles

z, km	Mixing ratio[a] H_2O (10^{-6})	H_2O_2 (10^{-12})	O_3 (10^{-6})	HNO_3 (10^{-9})	N_2O (10^{-8})	NO_2 (10^{-9})	HCl (10^{-9})	HOCl (10^{-11})
			September 26, 1989 (9 Limb Scans, 1105-1818 MDT, SZA=51.4°)					
37.51	5.25(0.42)	98.1(53.0)	7.16(0.42)	0.58(0.35)	3.72(0.42)	9.82(3.40)	2.04(0.18)	10.1 (2.47)
32.49	5.48(0.38)	118. (16.2)	8.71(0.46)	2.17(0.24)	8.68(0.79)	7.26(1.12)	1.87(0.16)	10.6 (1.0)
28.71	4.66(0.33)	68.7(18.1)	7.47(0.41)	4.18(0.43)	14.5(1.30)	2.84(1.22)	1.43(0.13)	7.36(0.90)
24.91	4.17(0.37)	11.2(12.5)	4.24(0.25)	6.56(0.66)	19.1(1.65)	1.49(0.97)	1.15(0.10)	3.31(0.68)
20.66	4.18(0.38)	20.9(11.6)	3.06(0.25)	5.37(0.54)	21.1(1.78)	0.88(1.24)	1.07(0.10)	0.88(0.60)
16.84	1.85(0.50)	19.9(151.)	0.79(1.51)	1.20(0.13)	29.5(2.52)	5.0 (11.9)	0.18(0.06)	...
			September 26-27, 1989 (13 Limb Scans, 2028-0337 MDT, Night Measurement)					
36.63	5.06(0.35)	101. (39.7)	7.28(0.42)	0.53(0.35)	4.12(0.45)	14.2 (2.6)	1.90(0.17)	12.9 (2.1)
31.72	5.13(0.36)	81.9(14.1)	8.45(0.44)	2.64(0.28)	9.22(0.84)	8.22(1.03)	1.76(0.15)	5.80(0.95)
27.91	4.75(0.32)	58.6(13.2)	6.73(0.37)	4.89(0.50)	15.1(1.35)	4.87(1.08)	1.28(0.11)	3.86(0.76)
24.40	4.91(0.34)	18.7(11.2)	5.21(0.30)	6.75(0.68)	18.7(1.36)	2.13(1.05)	1.28(0.11)	1.02(0.68)
20.36	3.47(0.36)	18.6(11.9)	1.78(0.21)	4.71(0.47)	22.4(1.88)	2.54(1.83)	0.81(0.09)	0.25(0.56)
15.96	2.30(0.60)	61.1(333.)	0.22(1.44)	0.64(0.07)	28.3(2.39)	...	0.07(0.05)	2.46(1.80)
			September 27, 1989 (3 Limb Scans, 1011-1235 MDT, SZA=43.5°)					
38.57	5.23(0.77)	...	7.14(0.52)	2.27(0.87)	1.97(0.53)	10.9 (4.6)	2.04(0.20)	6.54(4.11)
33.34	5.53(0.46)	75.0(27.4)	8.04(0.49)	1.69(0.25)	6.98(0.72)	5.79(1.65)	1.79(0.16)	11.6 (1.3)
29.87	5.21(0.41)	9.3(23.6)	7.94(0.48)	4.31(0.49)	10.6(1.10)	2.00(1.33)	1.67(0.15)	5.44(1.33)
25.63	4.71(0.35)	19.3(13.3)	5.42(0.33)	6.20(0.65)	12.2(1.17)	0.65(0.93)	1.27(0.12)	4.37(0.69)
21.96	4.50(0.39)	18.4(16.6)	2.47(0.25)	8.23(0.86)	16.6(1.56)	0.76(1.40)	1.44(0.13)	...
18.14	4.06(0.55)	...	2.70(0.87)	2.60(0.29)	22.7(2.89)	5.54(6.25)	0.49(0.07)	...

[a] 1σ errors include uncertainties from molecular parameters: H_2O (5%), H_2O_2 (2%), O_3 (5%), HNO_3 (10%), N_2O (8%), NO_2 (5%), HCl (8%), HOCl (3%).

Table 2. Time variation of OH and HO_2

Altitude, km	Mixing ratio[a] OH (10^{-12})	Mixing ratio[a] HO_2 (10^{-11})
September 26, 1989, 1105-1324 MDT, SZA=40.2°		
37.69	192. (22.)	19.1 (4.5)
32.78	34.8 (3.9)	7.75(1.36)
29.17	16.6 (3.1)	2.46(1.52)
25.22	-0.9 (1.8)	0.91(0.82)
20.49	1.1 (1.1)	0.47(0.62)
September 26, 1989, 1325-1559 MDT, SZA=47.1°		
37.43	160. (16.)	14.8 (3.7)
32.23	42.1 (4.0)	6.48(1.13)
28.19	12.7 (2.2)	5.59(1.02)
24.16	2.24(1.59)	1.60(0.79)
21.15	3.62(2.46)	0.72(1.28)
September 26, 1989, 1600-1811 MDT, SZA=67.0°		
37.08	98.1 (9.9)	10.0 (3.6)
33.16	20.9 (2.3)	4.80(1.08)
28.14	4.59(1.29)	3.61(0.87)
24.59	0.74(1.23)	...
20.55	0.88(1.19)	...
September 27, 1989, 1011-1235 MDT, SZA=43.5°		
38.57	183. (19.)	16.5 (4.2)
33.34	50.3 (4.7)	6.62(1.30)
29.87	15.6 (2.5)	7.42(1.12)
25.63	3.88(1.29)	1.87(0.63)
21.96	1.46(1.99)	1.25(0.72)

[a] 1σ errors include uncertainties from molecular parameters: OH (8%), HO_2 (2%).

uses the manifold of lines centered at 204.325 GHz for atmospheric retrievals. The data are reduced using both constrained least squares and sequential estimation fitting procedures [*Waters et al.*, 1984, 1988]. The radiative transfer calculation is also based on multilayered curved shell models of the atmosphere, with stratospheric temperature profiles derived from local radiosonde data. The 206.132-GHz O_3 line is used to calibrate instrument pointing. The estimated uncertainty for ClO includes random spectral noise, radiometric calibration errors, and spectral line parameter errors. The data presented here are an average of the ClO concentrations retrieved from 1100 MDT to 1600 MDT on September 26, 1989. During this time, little diurnal variation was seen or expected since ClO varies rapidly at sunrise and sunset but is relatively constant during midday [*de Zafra et al.*, 1987].

Results are presented for each species for the range of tangent heights that provide meaningful retrievals for the particular period of averaging. The results of the fitting and error analysis are presented in Tables 1, 2, and 3. Table 1 contains results from the first day average, the nighttime average, and the second day average. The sums for the second day include only observations made before the balloon began descending. Table 2 contains the OH and HO_2 retrievals for the four sets of short sums (three limb scans in each sum), three for the first day of the flight and one for the second day, which constitute the primary time-dependent measurements of HO_x from the present flight. The total FIRS-2 uncertainty estimate includes effects due to the following: nonlinear least squares fitting of the spectra, intensity calibration of the spectra, pointing errors, overhead abundance (discussed above), determination of ambient pressure, propagation of abundance uncertainties to lower layers in the onion-peeling process, and uncertainties in the molecular parameters (including their temperature uncertainties). Further laboratory measurements may improve the spectral line parameters enough to significantly decrease the systematic uncertainties for some molecules. The effect of diurnal variation of OH and HO_2 on the onion-peeling retrieval process (that is, concentrations in upper layers change during the limb-scanning process before observations at lower layers are completed) is found to be negligible for the present observations. Table 3 contains the BMLS measurements of ClO with 1σ errors that include all known systematic errors. Tables 1, 2, and 3 also include the measurement altitudes and average solar zenith angles for the locations of limb-sampling regions.

Photochemical Model

The observations are compared with the calculations made with a photochemical model constrained by measured concentrations of radical precursors [*Logan et al.*, 1978; *McElroy and Salawitch*, 1989; *Salawitch et al.*, 1994a]. Input to the model includes vertical profiles for O_3, NO_y (defined as the sum of [NO] + [NO_2] + [HNO_3] + [$ClNO_3$] + 2[N_2O_5] + [HNO_2] + [HNO_4]), Cl_y (defined as [Cl] + [ClO] + [HCl] + [$ClNO_3$] + [HOCl] + 2[Cl_2]), H_2O, CH_4, temperature, and aerosol surface area. We have obtained input profiles for O_3, H_2O, and temperature from an average of measure-

Table 3. BMLS ClO Mixing Ratio Profile

Altitude, km	ClO Mixing Ratio[a] (10^{-12})
September 26, 1989, 1100-1600 MDT, SZA=44°	
40.0	450.(80.)
35.0	410.(70.)
30.0	250.(50.)
25.0	73.(30.)
20.0	5.(30.)

[a] 1σ errors include uncertainties from molecular parameters.

ments for the first day, second day, and night, interpolated to a common altitude grid. The input profile for CH_4 is derived from FIRS-2 measurements of N_2O, using a relation developed from 1985 Atmospheric Trace MOlecule Spectroscopy (ATMOS) measurements [*Gunson et al.*, 1990], adjusted for the change in concentration of CH_4 between 1985 and 1989. NO_y is derived from the FIRS-2 measurements of N_2O using correlations measured by the ER-2 aircraft and by ATMOS [*Loewenstein et al.*, 1993; *Russell et al.*, 1988]. Total Cl_y is estimated from its relationship with N_2O based on measurements of chlorinated organic source gases [*Woodbridge et al.*, 1995] and is adjusted to match the chlorine levels in 1989. This relationship is consistent with ATMOS measurements of HCl and $ClNO_3$ [*Zander et al.*, 1990] as well as ATMOS measurements of chlorine source gases [*Zander et al.*, 1992] at the higher altitudes of the present measurements. The input profile of aerosol surface area peaks at 2×10^{-8} cm^{-1} at 16 km and is representative of nonvolcanic, background conditions based on measurements by the Stratospheric Aerosol and Gas Experiment II (SAGE II) (G.K. Yue, private communication, 1994). Thus to the extent feasible, the model reflects the state of the atmosphere at the time of the balloon flight, as determined from measurements of the long-lived species that are precursors to radicals and reservoir species. Using this set of input parameters, the model is used to calculate diurnally varying concentration profiles by balancing production and loss of each species over a 24-hour period [*Logan et al.*, 1978] using reaction rates and photolysis cross sections from the current Jet Propulsion Laboratory recommendation [*DeMore et al.*, 1994] (JPL94). A reaction probability of 0.1 is used for the heterogeneous hydrolysis of N_2O_5 (JPL94); the formulation of *Hanson et al.* [1994] is adopted for the rate of the heterogeneous hydrolysis of $ClNO_3$. A radiative transfer model that includes Rayleigh and aerosol scattering is used to calculate photolysis rates [*Prather*, 1981]. The calculated rate for photolytic production of O^1D from O_3 is based on a study that allows for production of O^1D via excited rovibrational states of O_3 [*Michelsen et al.*, 1994]. This rate leads to ~40% enhancements in O^1D production and ~15% enhancements in concentrations of OH in the lower stratosphere relative to models using the rate given by JPL94 but has a negligible effect on OH in the upper stratosphere. Additionally, the absorption cross sections for H_2O_2, HNO_4, and HNO_2 have been extrapolated to longer wavelengths than given in JPL94 in order to accurately represent photolysis of these molecules at high solar zenith angle (SZA).

Discussion

HO_x Species

Our midday measurements of OH fall within the range of the previous measurements shown in Figure 4 of *Pickett and Peterson* [1993]. The variations between our measurement and previous measurements are reasonable considering the accumulated errors and atmospheric variability with latitude and season. Present measurements of HO_2 in the stratosphere are in good agreement with previous measurements summarized by *Park and Carli* [1991]. The strengths of the present set of observations are the simultaneous measurement of the full HO_x chemical family during a full diurnal cycle, and the ability to compare these observations with a model constrained by simultaneous measurements of H_2O and O_3, which regulate concentrations of HO_x. Similar measurements have been made in the lower stratosphere from the NASA ER-2 during the Stratospheric Photochemistry, Aerosols and Dynamics Expedition (SPADE) mission [*Wennberg et al.*, 1994; *Salawitch et al.*, 1994a, 1994b]. The present work extends this type of comparison to an altitude range that includes most of the stratosphere.

Comparisons of concentrations of OH and HO_2 measured at four solar zenith angles and model calculations are shown in Figure 2. Measurements from Table 2 are plotted at the nearest corresponding altitudes used for modeling (solid circles) and are linearly interpolated vertically to provide values on the same altitude grid as the model calculations (38, 32, 28, and 24 km), to emphasize comparison of the solar zenith dependence between the data and the model and to remove the effects of different tangent altitudes in the various sums of limb-scan sequences. The interpolated values are plotted as open circles. The average SZAs for the measurements, which determine the average local solar time used in Figure 2, are calculated from the latitude, longitude, and viewing direction of the instrument.

Chi-square statistics are used to test the quality of the agreement between the interpolated measurements and photochemical model results by determining whether differences can be explained simply by random errors of the measurements. We assume for this purpose that the measurements are normally distributed around the actual values with the uncertainties representing the 1σ random errors of the measurements. Chi-square values are calculated as

$$\chi^2 = \sum_{i=1}^{n}((x_{meas}(i) - x_{model}(i))/\delta x(i))^2,$$

where n is the number of degrees of freedom, $x_{meas}(i)$ and $x_{model}(i)$ are measurements and modeled values, respectively, and $\delta x(i)$ is the 1σ measurement uncertainty. Chi-square comparisons are used only in cases where potential systematic uncertainties due to molecular line parameters are negligible.

With the exception of OH at 38 and 32 km and HO_2 at 28 km the χ^2 values for the HO_x measurements are all less than 4, with 4 degrees of freedom, suggesting a better than 50% probability of agreement between the measurements and the model. For the three with larger χ^2 values (23.05 for OH at 38 km, 12.56 for OH at 32 km, and 7.84 for HO_2 at 28 km) the diurnal trends for the theory and observation are consistent but the probabilities of agreement are small (less than 1%, 1.4%, and

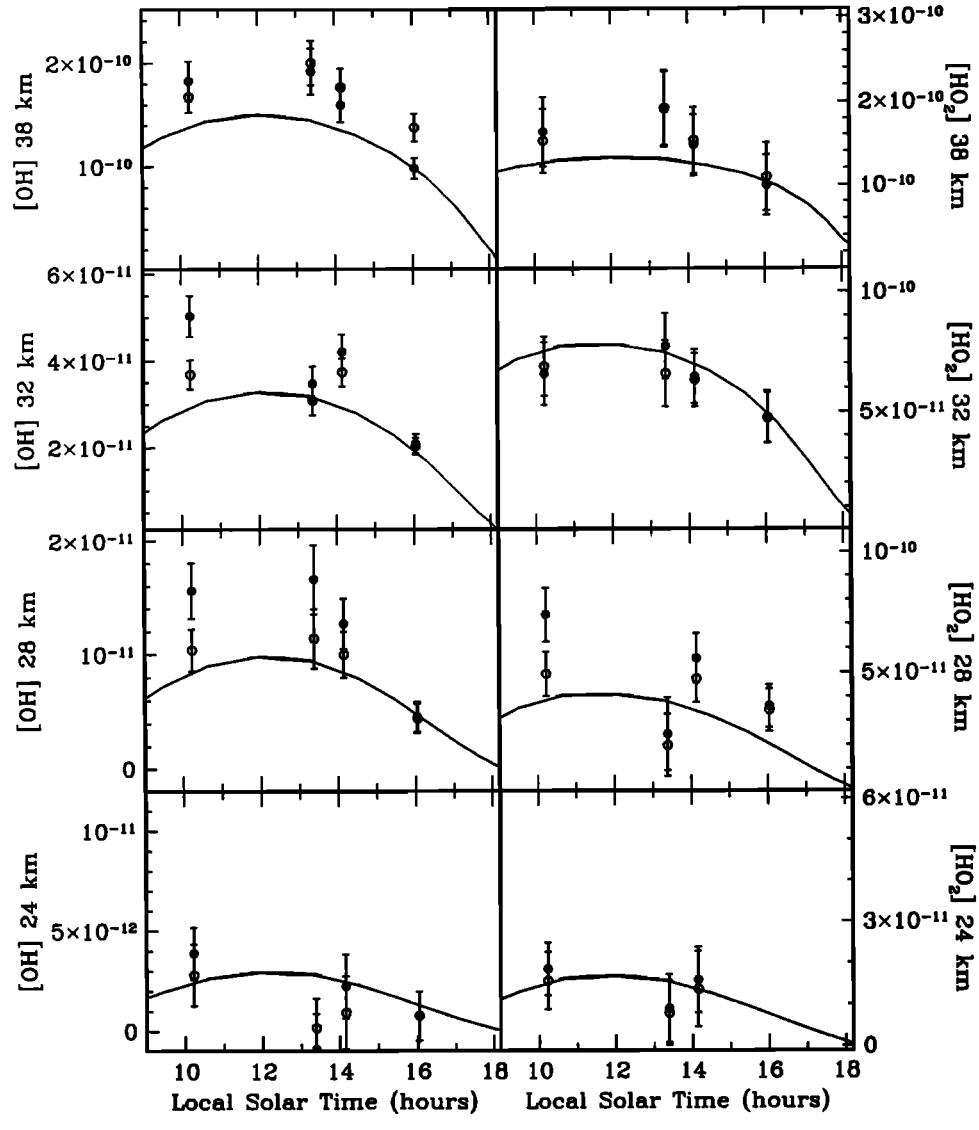

Figure 2. Measured and modeled OH and HO_2 concentrations versus solar zenith angle. Solid circles are the measured mixing ratios from Table 2, plotted at nearest corresponding altitudes of the modeling grid. Open circles are these concentrations linearly interpolated to the modeling grid altitudes of 38, 32, 28, and 24 km.

9.8% for the three cases, respectively). In particular, measurements of OH are significantly higher (~33%) than model values at 38 km. This difference is unlikely to be due to uncertainty in the UV flux and O_3 concentration involved in estimating the production of OH from the reaction of O^1D with H_2O since the model is constrained by the observed concentrations of O_3 (1σ uncertainties of 6-7% at this altitude) and the overhead column abundance of O_3 used in the model agrees with the column inferred from the measurements to within 10%.

Figure 3a compares the retrieved and calculated profiles of H_2O_2. Both the magnitude and the shape of the calculated profiles disagree with the data at about the 2σ level, implying that our current understanding of the relative creation ($HO_2 + HO_2 \rightarrow H_2O_2 + O_2$) and photolysis rates for H_2O_2 may be incomplete.

NO_y Species

Measurements of HNO_3 by FIRS-2 for this flight show very good agreement with previous balloon-borne remote and in situ measurements. Our measurements are consistent with observations of HNO_3 by the Balloon-borne Laser In Situ Sensor (BLISS) at 31 km in 1988 to within the error bars [*May and Webster*, 1989] and are also consistent with many previous measurements at similar latitudes summarized in Figure 3 of *May and Webster* [1989]. However, our observation of HNO_3 are consistently 30-40% higher than retrievals by ATMOS for the northern hemisphere [*Russell et al.*, 1988], especially for altitudes below 28 km. The most likely explanation for these differences is that the measurements were taken 4 years apart, in different seasons, and at slightly different latitudes. The ATMOS measure-

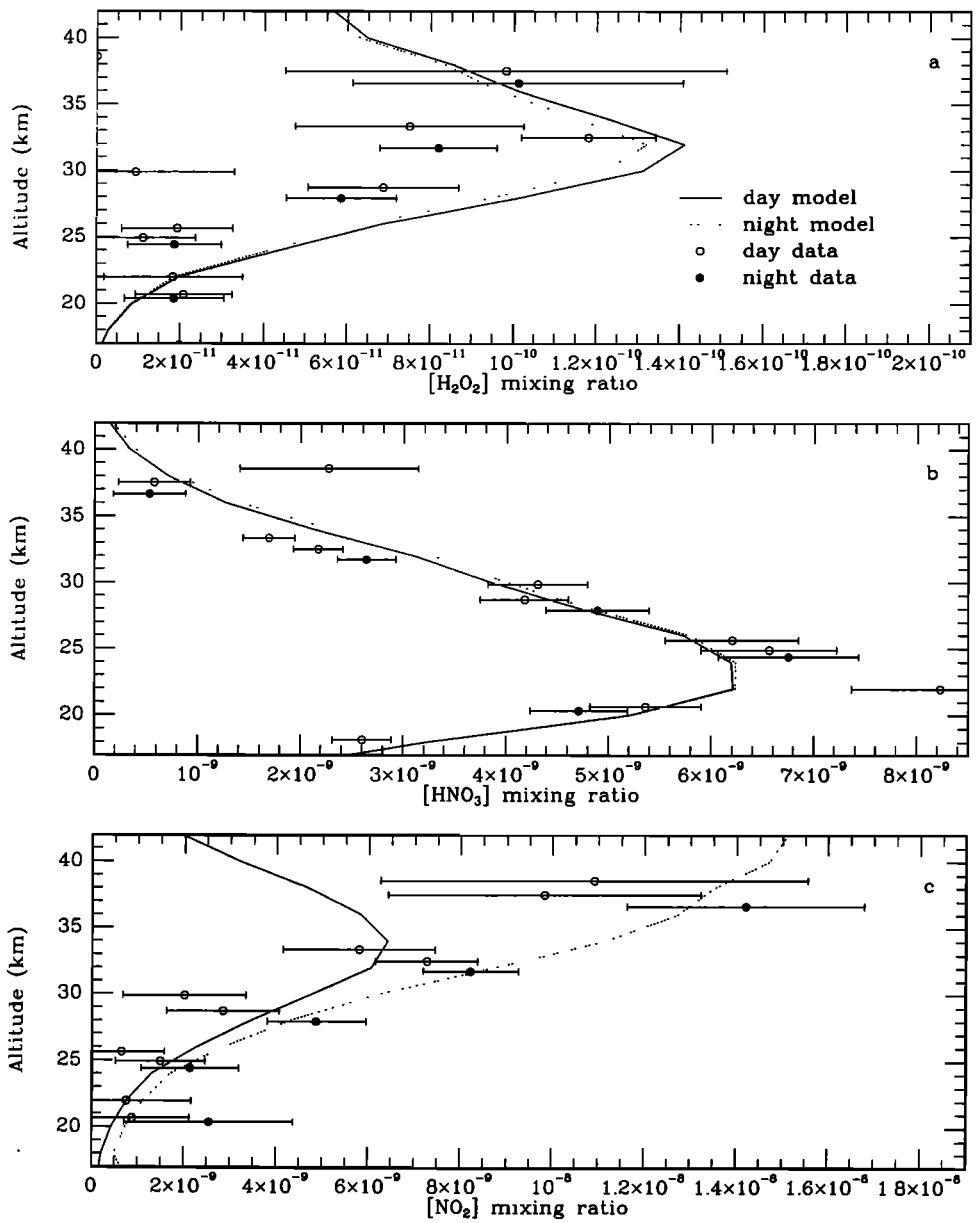

Figure 3. Far-Infrared Spectrometer (FIRS-2) balloon measurements from September 26-27, 1989, and corresponding model calculations. (a) H_2O_2, (b) HNO_3, (c) NO_2.

ments were obtained at slightly lower latitudes (~28°) than our measurements (32°-37°N), which could explain some of the discrepancy. The fact that different vibrational bands are used by FIRS-2 and ATMOS retrievals is unlikely to cause the discrepancy, since all previous balloon measurements, including BLISS, use the same vibrational bands for retrieval as ATMOS, and the uncertainties in band strengths are about 10% [*Goldman et al.*, 1975; *Giver et al.* 1984; *May et al.*, 1987].

Figure 3b compares measured and modeled profiles for HNO_3. The measurements are about 10-30% higher than the model at the peak of the mixing ratio profile, where HNO_3 comprises 50-70% of the total NO_y, and slightly lower than the model at the upper altitudes. Some of this discrepancy could be due to uncertainty in the spectroscopic transition intensity (~10%), which is included in the error analysis. Also, measurement uncertainties for O_3 and N_2O, used as inputs to the model, affect calculated HNO_3 at the 10% level. (N_2O is used to infer NO_y, which will have a direct effect on HNO_3.) Additionally, error in the NO_y/N_2O relationship could affect modeled HNO_3 in a similar manner. If the NO_y levels were higher, as suggested by the measurements of HNO_3, then the modeled levels of NO_2, ClO, and HO_x species near the peak of the HNO_3 mixing ratio profile would be significantly different.

The FIRS-2 daytime observations of NO_2, shown in Figure 3c, differ slightly from previous observations [*Webster et al.*, 1990; *Russell et al.*, 1988] and from model profiles. Our measurements in the 37 to 40 km re-

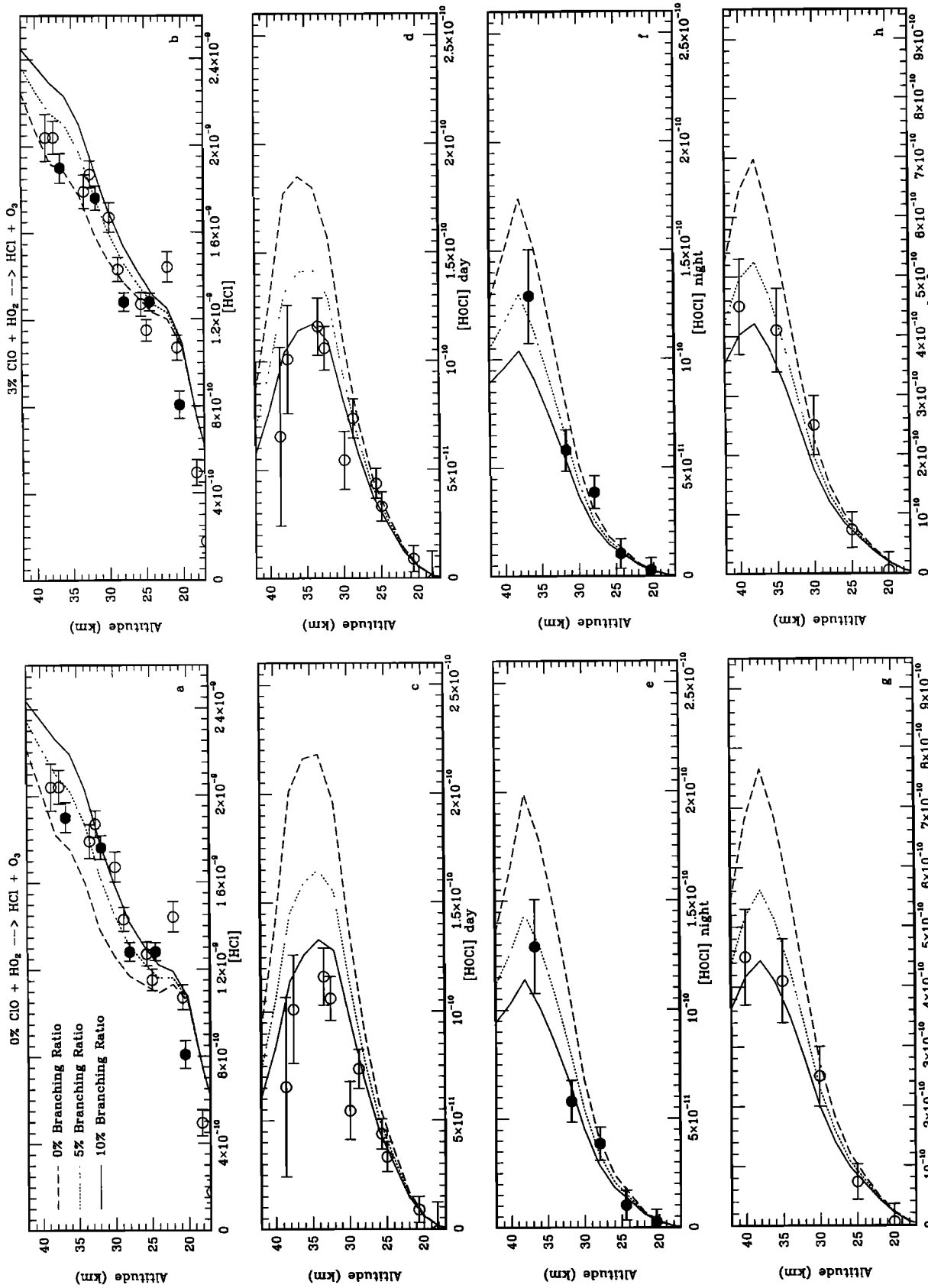

Figure 4. FIRS-2 and Balloon Microwave Limb Sounder (BMLS) balloon measurements from September 26-27, 1989, for Cl_y species and corresponding model calculations using varying branching ratios for the reactions of ClO with OH and HO_2 to produce HCl.

gion are consistently $\sim 1\sigma$ higher than the previously reported measurements and model values. The nighttime measurements agree well with the model. The ability of FIRS-2 to measure NO_2 was limited at the time of this balloon flight, making it difficult to draw more definite conclusions from the comparison. Improved measurements of NO_2, enabled by improved noise performance in the far-infrared channel, will become available from more recent FIRS-2 flights. This will permit more detailed evaluation of NO_y partitioning.

Cl_y Species

Recently reported measurements of HCl and ClO from the Submillimeter Limb Sounder (SLS) [*Stachnik et al.*, 1992] show that the ClO/HCl ratio is much lower than suggested by photochemical models. Investigations of ATMOS measurements of HCl and $ClNO_3$ similarly indicate that the $ClNO_3$/HCl ratio is lower than expected [*Natarajan and Callis*, 1991; *Minschwaner et al.*, 1993; *H.A. Michelsen*, unpublished results, 1994]. One proposal that would explain this is that ClO and OH react to produce HCl, as suggested by *McElroy and Salawitch* [1989]. JPL94 suggests a lower limit of 0% for the HCl branching ratio, with an upper limit of 14%, since production of HCl is a four-center reaction involving the breaking and making of multiple chemical bonds. Similarly, the possibility of production of HCl from the reaction of ClO + HO_2 may also be important for resolving the discrepancy (the JPL94 recommended branching ratio is 0% with an upper limit of 3%). Uncertainties in the photolysis of HOCl are not responsible for this discrepancy since HOCl has been shown to be a good proxy for ClO when measured simultaneously with HO_2, OH, and O_3 [*Johnson et al.*, 1995b]. Also, in the comparison shown below, HOCl and ClO are both lower than model calculations; uncertainties in the photolysis cross sections would affect them in opposite senses.

The set of measurements from this balloon flight is ideally suited for addressing partitioning within the Cl_y family. Besides the direct measurement of ClO, HCl, and HOCl, we also measure concentrations of most of the reactants (OH, HO_2, and NO_2) involved in the creation and destruction of the main reservoir species in the Cl_y family. The only important species not measured is CH_4, whose reaction with Cl is the main source of HCl. CH_4 can be estimated quite accurately from its

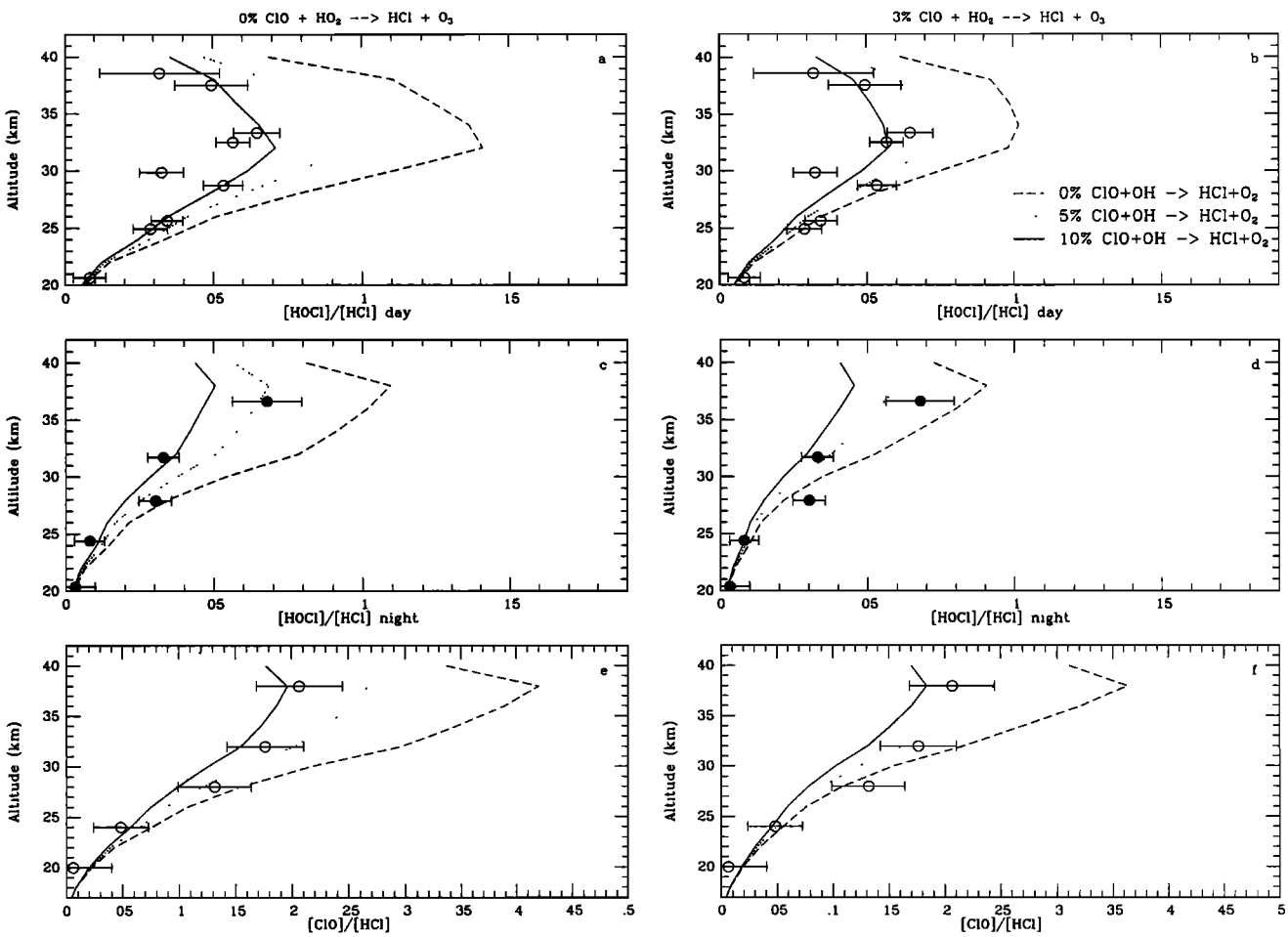

Figure 5. Comparisons of measured and modeled [HOCl]/[HCl] and [ClO]/[HCl] ratios, assuming various branching ratios of the reactions of ClO with OH and HO_2 to produce HCl. The measured ClO and HCl concentrations are interpolated onto the altitude grid of the model.

observed correlations with N_2O [*Gunson et al.*, 1990; *M.R. Gunson*, private communication, 1990]. The main sink for HCl is its reaction with OH to produce Cl + H_2O. As stated earlier, the modeled OH agrees well with the measured OH except at the highest measurement altitudes, suggesting that the loss rate of HCl should be well described by the model assuming the validity of the current rate constant for OH + HCl. Especially given the high measured [OH] at 38 km, a very substantial decrease in the OH + HCl reaction rate would be required to explain the observed HCl. Uncertainties in OH do not provide an explanation for discrepancies in Cl_y in the present data set.

Figure 4 shows our measurements of three Cl_y species along with model calculations, corresponding to the average SZA of the measurements, assuming different branching ratios for the production of HCl from the reaction of ClO with both OH and HO_2. The left-hand side of the figure shows results from models incorporating a 0% branching ratio for the ClO + HO_2 reaction, and the right-hand side shows results for a 3% branching ratio. Each panel shows three model calculations, assuming branching ratios for the ClO + OH reaction of 0%, 5%, and 10%. Assuming the total Cl_y used in the model is correct, these plots suggest that there must be some production of HCl at the expense of ClO and HOCl, possibly through one or both of these mechanisms. We have found that inclusion of these alternate branching ratios has a negligible effect on HO_x and NO_x, as determined from direct comparison of model results.

To quantify the amount of any additional HCl production (and loss of ClO and HOCl) and to remove the uncertainty associated with model estimates of total Cl_y, we have plotted the ratios of [ClO]/[HCl] and [HOCl]/[HCl] (day and night) in Figure 5 using the same set of model branching ratios as in Figure 4. A statistical comparison of the measured ratios above 20 km and the model calculations shows improvement in the agreement with enhanced HCl production from both mechanisms, up to limits for the production of HCl given by the JPL94 recommendation. The best agreement is $\chi^2 = 29$ for 16 degrees of freedom, corresponding to a 2.5% confidence limit, obtained for 10% production of HCl from ClO + OH and 0% production of HCl from ClO + HO_2; similar results are obtained for 5% HCl production from ClO + OH and 3% HCl production from ClO + HO_2 and for 10% HCl production from ClO + OH and 3% HCl production from ClO + HO_2. (The 16 degrees of freedom correspond to the number of measurement points above 20 km; the [ClO/[HCl] in Figure 5 are actually shown on the model grid since they were measured at different altitudes and interpolated to this common grid for comparison.) These results are consistent with the conclusions from the recent SLS results [*Stachnik et al.*, 1992; *Toumi and Bekki*, 1993] as well as the ongoing analysis of ATMOS data [*H.A. Michelsen*, unpublished results, 1994]. The sensitivity of the measurements is not sufficient to make firm conclusions about the extent of HCl production from the reaction with HO_2 relative to the reaction with OH. However, our observations indicate that production of HCl occurs by some process other than the reaction of Cl with CH_4.

Conclusions

We now have the most extensive set of measurements obtained to date of stratospheric radical species from the HO_x, Cl_x, and NO_x families and a number photochemically related gases. An atmospheric model constrained by measurements of long-lived radical precursors enables us to critically examine processes that regulate the abundance of radicals.

We have found HO_x concentrations that are largely in agreement with the model values, except for OH at the highest measurement altitudes, near 38 km. Concentrations of H_2O_2 are consistent with calculated values for 30 km and above.

Daytime concentrations of NO_2 are somewhat higher than model values at the highest measurement altitudes, and nighttime concentrations are in good agreement. Concentrations of HNO_3 are higher than model values near 25 km and slightly lower at altitudes above 32 km. The partitioning of NO_y agrees with the model to within the limited measurement capability for NO_2 at the time of this flight.

The major discrepancy between the measurements and standard model calculations is for the chlorine species HCl, ClO, and HOCl. We find concentrations of HCl to be higher and concentrations of ClO and HOCl to be lower than those calculated with the model. The discrepancy could be explained by small branching ratios to form HCl in the reactions of ClO with OH and/or HO_2. Uncertainty in the main HCl loss term, reaction with OH, implied by uncertainty in the OH concentration, can be ruled out as the cause of this discrepancy.

The measurement set includes most of the radical species involved in the rate-determining steps for catalytic ozone loss [*Wennberg et al.*, 1994]. Detailed comparisons are currently in progress of the contributions of the different radical families over the wide range of altitudes sampled by the FIRS-2 and BMLS instruments to photochemical loss of ozone and concurrent ozone production.

Acknowledgments. We are grateful to the Jet Propulsion Laboratory Atmospheric Ballooning Group for furnishing and supporting the gondola and to the National Scientific Balloon Facility for the balloon launch services. The work was supported by NASA grants NSG-5175 (SAO) and NAGW-1230 (Harvard University). H.A. Michelsen was supported by an NSF Postdoctoral Research Fellowship. Part of this research was performed at the Jet Propulsion Laboratory, California Institute of Technology, under contract with NASA.

References

Anderson, J.G., H.J. Grassl, R.E. Shetter, and J.J. Margitan, HO_2 in the stratosphere: Three in situ observations, *Geophys. Res. Lett.*, *8*, 289-292, 1981.

Avallone, L.M., D.W. Toohey, M.H. Proffitt, J.J. Margitan, K.R. Chan, and J.G. Anderson, In situ measurements of ClO at mid-latitudes: Is there an effect from Mt. Pinatubo? *Geophys. Res. Lett., 20,* 2519-2522, 1993.

Burnett, C.R., K.R. Minschwaner, and E.B. Burnett, Vertical column abundance measurements of atmospheric hydroxyl from 26°, 40°, 65° N, *J. Geophys. Res., 93,* 5341-5253, 1988.

Carli, B., B.M. Dinelli, F. Mencaraglia, and J.H. Park, The mixing ratio of the stratospheric hydroxyl radical from far infrared emission measurements, *J. Geophys. Res., 94,* 11,049-11,058, 1989.

Chance, K.V., and W.A. Traub, Evidence for stratospheric hydrogen peroxide, *J. Geophys. Res., 92,* 3061-3066, 1987.

Chance, K.V., D.G. Johnson, and W.A. Traub, Measurement of stratospheric HOCl: Concentration profiles, including diurnal variation, *J. Geophys. Res., 94,* 11,059-11,069, 1989.

Chance, K.V., D.G. Johnson, W.A. Traub, and K.W. Jucks, Measurement of the stratospheric hydrogen peroxide concentration profile using far-infrared thermal emission spectroscopy, *Geophys. Res. Lett., 18,* 1003-1006, 1991.

Chance, K., K.W. Jucks, D.G. Johnson, and W.A. Traub, The Smithsonian Astrophysical Observatory database SAO92, *J. Quant. Spectrosc. Radiat. Transfer, 52,* 447-457, 1994.

DeMore, W.B., S.P. Sander, D.M. Golden, R.F. Hampson, M.J. Kurylo, C.J. Howard, A.R. Ravishankara, C.E. Kolb, and M.J. Molina, Chemical kinetics and photochemical data for use in stratospheric modeling, in Evaluation 11, *JPL Publ. 94-26,* Jet Propul. Lab., Pasadena, Calif, 1994.

Dessler, A.E., et al., Balloon-borne measurements of ClO, NO, and O_3 in a volcanic cloud: An analysis of heterogeneous chemistry between 20 and 30 km, *Geophys. Res. Lett., 20,* 2527-2530, 1993.

de Zafra, R.L., A. Parrish, P.M. Solomon, and J.W. Barrett, A measurement of stratospheric HO_2 by ground-based millimeter-wave spectroscopy, *J. Geophys. Res., 89,* 1321-1326, 1984.

de Zafra, R.L., M. Jaramillo, A. Parrish, P. Solomon, B. Connor, and J. Barrett, High concentrations of chlorine monoxide at low altitudes in the Antarctic spring stratosphere: Diurnal variation, *Nature, 328,* 408-411, 1987.

Emmons, L.K., D.T. Shindell, J.M. Reeves, and R.L. de Zafra, Stratospheric ClO profiles from McMurdo Station, Antarctica, spring 1992, *J. Geophys. Res., 100,* 3049-3055, 1995.

Giver, L.P., F.P.J. Valero, D. Goorvitch, and F.S. Bonomo, Nitric-acid band intensities and band-model parameters from 610 to 1760 cm^{-1}, *J. Opt. Soc. Am. B, 1,* 715-722, 1984.

Goldman, A., F.S. Bonomo, W.J. Williams, and D.G. Murcray, Statistical-band-model analysis and integrated intensity for the 21.8 μm bands of HNO_3 vapor, *J. Opt. Soc. Am., 65,* 10-12, 1975.

Gunson, M.R., C.B. Farmer, R.H. Norton, R. Zander, C.P. Rinsland, J.H. Shaw, and B.-C. Gao, Measurements of CH_4, N_2O, CO, H_2O and O_3 in the middle atmosphere by the Atmospheric Trace Molecule Spectroscopy experiment on Spacelab 3, *J. Geophys. Res., 95,* 13,867-13,882, 1990.

Hanson, D.R., A.R. Ravishankara, and S. Solomon, Heterogeneous reactions in sulfuric acid aerosols: A framework for model calculation, *J. Geophys. Res., 99,* 3615-3630, 1994.

Heaps, W.S., and T.J. McGee, Progress in stratospheric hydroxyl measurements by balloon-borne lidar, *J. Geophys. Res., 90,* 7913-7921, 1985.

Helten, M., W. Pätz, M. Trainer, H. Fark, E. Klein, and D.H. Ehhalt, Measurements of stratospheric HO_2 and NO_2 by matrix isolation and ESR spectroscopy, *J. Atmos. Chem., 2,* 191-202, 1984.

Iwagami, N., S. Inomata, I. Murata, and T. Ogawa, Doppler detection of hydroxyl column abundance in the middle atmosphere, *J. Atmos. Chem., 20,* 1-15, 1995.

Johnson, D.G., K.W. Jucks, W.A. Traub, and K.V. Chance, The Smithsonian stratospheric far-infrared spectrometer and data reduction system, *J. Geophys. Res., 100,* 3091-3106, 1995a.

Johnson, D.G., W.A. Traub, K.V. Chance, and K.W. Jucks, Estimating the abundance of ClO from simultaneous remote sensing measurements of HO_2, OH, and HOCl, *Geophys. Res. Lett., 22,* 1869-1871, 1995b.

Kendall, D.J.W., and T.A. Clark, Stratospheric observation of far IR pure rotational lines of hydroxyl, *Nature, 283,* 57-58, 1980.

Loewenstein M., et al., New observations of the NO_y/N_2O correlation in the lower stratosphere, *Geophys. Res. Lett., 20,* 2531-2534, 1993.

Logan, J.A., M.J. Prather, S.C. Wofsy, and M.B. McElroy, Atmospheric chemistry: Response to human influence, *Phil. Trans. R. Soc. A, 290,* 187-234, 1978.

May, R.D., and C.R. Webster, In situ stratospheric measurements of HNO_3 and HCl near 30 km using the Balloon-borne Laser In Situ Sensor tunable diode laser spectrometer, *J. Geophys. Res., 94,* 16,343-16,350, 1989.

May, R.D., C.R. Webster, and L.T. Molina, Tunable diode laser measurements of absolute linestrengths in the HNO_3 ν_2 band near 5.8 μm, *J. Quant. Spectrosc. Radiat. Transfer, 38,* 381-388, 1987.

McElroy, M.B., and R.J. Salawitch, Changing composition of the global stratosphere, *Science, 243,* 763-770, 1989.

Michelsen, H.A., R.J. Salawitch, P.O. Wennberg, and J.G. Anderson, Production of $O(^1D)$ from photolysis of O_3, *Geophys. Res. Lett., 21,* 2227-2230, 1994.

Minschwaner, K., R.J. Salawitch, and M.B. McElroy, Absorption of solar radiation by O_2: Implications for O_3 and lifetimes of N_2O, $CFCl_3$, and CF_2Cl_2, *J. Geophys. Res., 98,* 10,543-10,561, 1993.

Natarajan, M., and L.B. Callis, Stratospheric photochemical studies with Atmospheric Trace Molecule Spectroscopy (ATMOS) measurements, *J. Geophys. Res., 96,* 9361-9370, 1991.

Park, J.H., and B. Carli, Spectroscopic measurement of HO_2, H_2O_2, and OH in the stratosphere, *J. Geophys. Res., 96,* 22,535-22,541, 1991.

Pickett, H.M., and D.B. Peterson, Stratospheric OH measurements with a far-infrared limb observing spectrometer, *J. Geophys. Res., 98,* 20,507-20,515, 1993.

Prather, M.J., Ozone in the upper stratosphere and mesosphere, *J. Geophys. Res., 86,* 5325-5338, 1981.

Roscoe, H.K., et al., Intercomparison of remote measurements of stratospheric NO and NO_2, *J. Atmos. Chem., 10,* 111-144, 1990.

Russell, J.M., III, C.B. Farmer, C.P. Rinsland, R. Zander, L. Froidevaux, G.C. Toon, B. Gao, J. Shaw, and M. Gunson, Measurements of odd nitrogen compounds in the stratosphere by the ATMOS experiment on Spacelab 3, *J. Geophys. Res., 93,* 1718-1736, 1988.

Salawitch, R.J., et al., The distribution of hydrogen, nitrogen and chlorine radicals in the lower stratosphere: Implications for changes in O_3 due to emission of NO_y from supersonic aircraft, *Geophys. Res. Lett., 21,* 2547-2550, 1994a.

Salawitch, R.J., et al., The diurnal variation of hydrogen, nitrogen and chlorine radicals: Implications for the heterogeneous production of HNO_2, *Geophys. Res. Lett., 21,* 2554-2550, 1994b.

Stachnik, R.A., J.C. Hardy, J.A. Tarsala, and J.W. Waters,

Submillimeterwave heterodyne measurements of stratospheric ClO, HCl, O_3, and HO_2: First results, *Geophys. Res. Lett., 19,* 1931-1934, 1992.

Stimpfle, R.M., P.O. Wennberg, L.B. Lapson, and J.G. Anderson, Simultaneous, in situ measurements of OH and HO_2 in the stratosphere, *Geophys. Res. Lett., 17,* 1905-1908, 1990.

Toon, G.C., C.B. Farmer, P.W. Schaper, L.L. Lowes, and R.H. Norton, Composition measurements of the 1989 Arctic winter stratosphere by airborne infrared solar absorption spectroscopy, *J. Geophys. Res., 97,* 7939-7961, 1992.

Toumi, R., and S. Bekki, The importance of the reactions between OH and ClO for stratospheric ozone, *Geophys. Res. Lett., 20,* 2447-2450, 1993.

Traub, W.A., D.G. Johnson, and K.V. Chance, Stratospheric hydroperoxyl measurements, *Science, 247,* 446-449, 1990.

Traub, W.A., K.V. Chance, D.G. Johnson, and K.W. Jucks, Stratospheric spectroscopy with the far-infrared spectrometer (FIRS-2): Overview and recent results, *Proc. Soc. Photo Opt. Instrum. Eng., 1491,* 298-307, 1991.

Waters, J.W., J.C. Hardy, R.F. Jarnot, H.M. Pickett, and P. Zimmermann, A balloon-borne microwave limb sounder for stratospheric measurements, *J. Quant. Spectrosc. Radiat. Transfer, 32,* 407-433, 1984.

Waters, J.W., R.A. Stachnik, J.C. Hardy, and R.F. Jarnot, ClO and O_3 stratospheric profiles: Balloon microwave measurements, *Geophys. Res. Lett., 15,* 780-783, 1988.

Waters, J.W., L. Froidevaux, W.G. Read, G.L. Manney, L.S. Elson, D.A. Flower, R.F. Jarnot, and R.S. Harwood, Stratospheric ClO and ozone from the microwave limb sounder on the Upper Atmosphere Research Satellite, *Nature, 362,* 597-602, 1993.

Webster, C.R., R.D. May, R. Toumi, and J.A. Pyle, Active nitrogen partitioning and the nighttime formation of N_2O_5 in the stratosphere: Simultaneous in situ measurements of NO, NO_2, HNO_3, O_3, and N_2O using the BLISS diode laser spectrometer, *J. Geophys. Res., 95,* 13,851-13,866, 1990.

Wennberg, P.O., R.M. Stimpfle, E.M. Weinstock, A.E. Dessler S.A. Lloyd, L.B. Lapson, J.J. Schwab, and J.G. Anderson, Simultaneous, in situ measurements of OH and HO_2, O_3, and H_2O: A test of modeled stratospheric HO_x chemistry, *Geophys. Res. Lett., 17,* 1909-1912, 1990.

Wennberg, P.O., et al., Removal of stratospheric O_3 by radicals: In situ measurements of OH, HO_2, NO, NO_2, ClO, and BrO, *Science, 266,* 398-404, 1994.

Woodbridge, E.L., et al., Estimates of total organic and inorganic chlorine in the lower stratosphere from in situ and flask measurements during AASE II, *J. Geophys. Res., 100,* 3057-3064, 1995.

World Meteorological Organization (WMO), Atmospheric ozone 1985: Assessment of our understanding of the processes controlling its present distribution and change, *WMO Rep. 16,* Global Ozone Res. and Monit. Proj., Geneva, 1986.

World Meteorological Organization, Report of the International Ozone Trends Panel 1988, Geneva, 1989.

Zander, R., M.R. Gunson, J.C. Foster, C.P. Rinsland, and J. Namkung, Stratospheric $ClONO_2$, HCl, and HF concentration profiles derived from Atmospheric Trace Molecule Spectroscopy experiment Spacelab 3 observations: An update, *J. Geophys. Res., 95,* 20,519-20,525, 1990.

Zander, R., M.R. Gunson, C.B. Farmer, C.P. Rinsland, F.W. Irion, and E. Mahieu, The 1985 chlorine and fluorine inventories in the stratosphere based on ATMOS observations at 30° north latitude, *J. Atmos. Chem., 15,* 171-186, 1992.

K. Chance, P. Ciarpallini, D. G. Johnson, K. W. Jucks, and W. A. Traub, Harvard-Smithsonian Center for Astrophysics, 60 Garden Street, Cambridge, MA 02138

R. A. Stachnik, Jet Propulsion Laboratory, 4800 Oak Grove Drive, Pasadena, CA 91109

H. A. Michelsen and R. J. Salawitch, Department of Earth and Planetary Sciences, Harvard University, Cambridge, MA 02138

(Received January 12, 1995; revised December 13, 1995; accepted December 13, 1995.)